ARTICLE

Microarrays Made Easy: Biofunctionalized Hydrogel Channels for Rapid Protein Microarray Production

Victoria de Lange, Andreas Binkert, Janos Vörös, and Marta Bally*,†

Laboratory of Biosensors and Bioelectronics, Institute for Biomedical Engineering, University and ETH Zurich, Gloriastrasse 35, 8092 Zurich, Switzerland

ABSTRACT We present a simple, inexpensive, and sensitive technique for producing multiple copies of a hydrogel-based protein microarray. An agarose block containing 25 biofunctionalized channels is sliced perpendicularly to produce many identical biochips. Each microarray consists of 500 μm spots, which contain protein-coated microparticles physically trapped in porous SeaPrep agarose. Proteins diffuse readily through SeaPrep agarose, while the larger microparticles are immobilized in the hydrogel matrix. Without major assay optimization, the limit of detection is 12 pM for a sandwich assay detecting human IgG. These highly flexible, multiplexed arrays can be produced rapidly without any special instrumentation and are compatible with standard fluorescence-based read-out.

KEYWORDS: protein microarray • microparticle-based assay • hydrogel • agarose • microchannel

1. INTRODUCTION

Spatially addressable spots of biomolecules can be immobilized in a dense pattern to create arrays of miniature test sites. These microarrays allow researchers to monitor biorecognition reactions in parallel, providing a wealth of biological information in a short processing time (1, 2). DNA microarrays are already well-established for analyzing nucleic acids but provide limited information about protein expression and functionality (3−6). Protein microarrays can improve our understanding of disease pathways (7) and lead to drug target and biomarker discovery (1, 3). The importance of protein biomarkers for making an early diagnosis, accurately identifying disease types, and assessing the response to treatment continues to motivate research in this area (8).

The fragile nature of proteins makes it difficult to immobilize them on a solid support without compromising their bioactivity (8). Unlike nucleic acids, which can be stored for extended periods in dry conditions, keeping proteins in a liquid environment is essential for preserving their structure and, consequently, their biological function (5, 9, 10). Two-dimensional (2D) activated glass slides (e.g., epoxy or aldehyde) are commonly used to immobilize proteins through covalent or electrostatic interactions (11−13). While biomolecule attachment is strong and localized on these slides, the capture proteins tend to suffer from drying or surface induced conformational changes (12). As an alternative, three-dimensional (3D) supports increase the binding capacity and attempt to preserve protein function, typically by immobilizing proteins in a hydrophilic environment (10, 14). Common 3D supports include the following: nitrocellulose (15), SuperProtein (hydrophobic polymer) (12), and hydrogels, such as poly(ethyl glucose) (PEG) (16, 17), polyacrylamide and modified polyacrylamide (18−20), poly(vinyl alcohol) (PVA) (17, 21), polyurethane (22), carboxymethylated dextran (23), and agarose (17, 24).

Hydrogels provide an aqueous environment for biological interactions (10), and their use in microarrays has shown increased sensitivity compared to planar surfaces (14, 25). Many hydrogels have low background fluorescence, making them well-suited for standard fluorescence-based read-out systems, such as microscopes or confocal scanners (6, 26).

Guschin et al. first reported a hydrogel microarray where proteins are immobilized in microfabricated polyacrylamide gel pads (27, 28). Since then, several techniques have been reported using patterns of hydrogels to array biomolecules (e.g., proteins (23, 27, 29−32), enzymes (29), oligonucleotides (27), or small molecules (32)). Photopatterning of hydrogels has also been combined with microfluidics to monitor enzymatic reactions (33, 34). Another approach to patterning hydrogels uses automated robotic spotting to create biomolecule-loaded hemispherical drops on a planar surface (10, 14, 17, 35−38).

One method of biofunctionalizing hydrogels is to incorporate microparticles into the matrix as protein supports (13, 17, 34, 39). These bead-based systems have a high degree of flexibility for ligand choice and capture probe immobilization (4, 41−43). Using microparticles, it is possible to optimize protein attachment for each array element and to test protein functionality before preparing the array (13, 43, 44). Additionally, proteins can be coupled to beads in an aqueous environment, preventing loss of functionality caused by drying (13). Integrating microparticles into the

* Corresponding author. E-mail: bally@chalmers.se.

Received for review September 8, 2010 and accepted November 12, 2010

† Current address: Department of Applied Physics, Chalmers University of Technology, Gothenburg, Sweden.

DOI: 10.1021/am100849f

Published on Web 12/09/2010

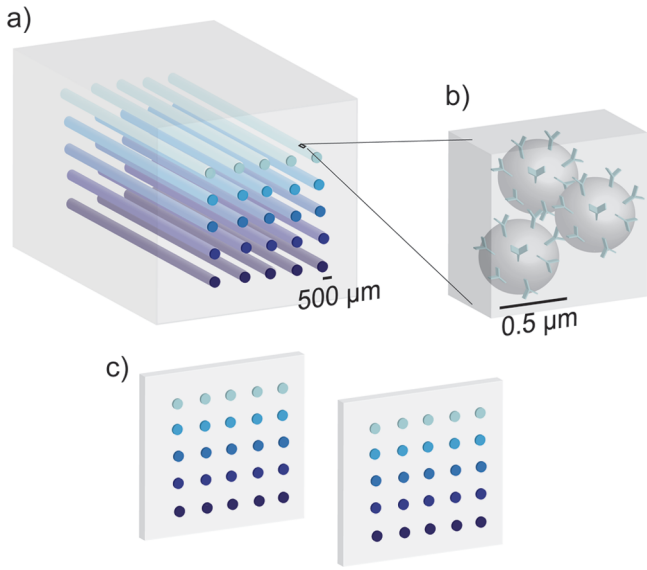

FIGURE 1. Schematic of the hydrogel microarray design. (a) The block of agarose contains 25 microchannels. (b) The channels are filled with functionalized microparticles immobilized in SeaPrep agarose. (c) The arrays are sliced perpendicular to the channels, creating multiple copies of the hydrogel-based protein microarray.

array also increases the surface area available for biorecognition reactions and can improve assay sensitivity (17, 42).

Microarrays are typically manufactured using robotic spotting or photolithography. Robotic spotting is a serial process, which can suffer from carry-over and drying problems. The lithographic methods are sophisticated and expensive techniques which require access to appropriate microfabrication facilities (40). We and others previously proposed a simple and cost-effective method to produce multiple biochip copies using standard laboratory equipment (39). The arrays are formed by cutting a structured hydrogel stack into thin slices.

In this paper, we use the hydrogel cutting technique to obtain highly flexible, multiplexed microarrays. To create the arrays, we injected a biofunctionalized hydrogel into microchannels (Figure 1). The channels were formed using a mold to gel an agarose block around an array of pins. Polystyrene microparticles were functionalized with immunoglobulins (IgGs) and combined with low gelation temperature SeaPrep agarose to fill the channels.

Agarose is a thermoreversible gel commonly used in electrophoresis, immunology, and as a culture medium for cells and other microorganisms (45). This hydrogel is well-suited to our system because it is protein resistant (45) and affordable (10) and has low fluorescent background (10) and a large pore size (45−47). The pore size of SeaPrep agarose allows antibody diffusion, while keeping microparticles immobilized (47).

We demonstrate the ease of array fabrication, without any specialized instrumentation, and the compatibility of our system with standard fluorescence read-out techniques (6). Using channels, we can create custom two-dimensional arrays and probe positioning is no longer limited to stripes, as it was in the layer-by-layer approach. The channel-based system is, therefore, more flexible, requires less material, and maintains the advantages of rapid and inexpensive array fabrication. Furthermore, the spot material and the surrounding gel can be individually tuned for optimized performance. A model reverse phase assay shows the multiplexing ability of our arrays, with low cross-reactivity and low unspecific binding. The limit of detection for a model sandwich assay was consistent with standard fluorescent bioanalytical assays (8). As an additional feature, we present the possibility of drying our microarrays to concentrate the fluorescent probes on a planar surface and further increase assay sensitivity.

2. EXPERIMENTAL METHODS

2.1. Materials. The following antibodies were purchased from Sigma, Switzerland: antihuman IgG (Fc specific, produced in goat), human IgG, antihuman IgG-FITC (fluorescein isothiocyanate; Fab specific, produced in goat), mouse IgG, and rabbit IgG. Alexa Fluor 488 antirabbit IgG (produced in goat) and Alexa Fluor 633 antimouse IgG (produced in goat) were from Invitrogen, Switzerland. Rabbit IgG-FITC and human IgG-FITC were from Sigma, Switzerland. Fluka agarose for molecular biology (gelling temperature: 34−37 °C) was used for the array support structure (Sigma, Switzerland, #05066). Ultra low gelling SeaPrep agarose (gelling temperature: <17 °C; melting temperature: 40−50 °C) was used to fill the channels (Lonza, Switzerland). Polybead carboxylated 0.5 μm polystyrene microspheres were embedded in the channels for biological assays (Polysciences GmbH, Germany). The surface of the particles was blocked with bovine serum albumin (BSA; ≥98%, Sigma-Aldrich, Switzerland). All arrays were prepared in a HEPES buffer solution, consisting of 10 mM 4-(2-hydroxyethyl) piperazine-1-ethane sulfonic acid (Sigma-Aldrich, Switzerland) and 150 mM NaCl, with the pH adjusted to 7.4.

2.2. Array Preparation. The channel support structure was prepared by dissolving agarose in HEPES buffer (3% w/v) while applying constant heat. The melted agarose was immediately injected into a mold using a syringe (both preheated to 45 °C). The mold is a metal chamber containing an array of 25 pins. The pins are 2 cm long and 500 μm in diameter and are arranged in rows of five. The support structure gelled around the pins for 20 min at room temperature. The pins were then gently extracted from the gel block and replaced with an addressing plate. The addressing plate has graduated channels from 700 to 500 μm for injecting the hydrogel/particle mixture with a pipet. A detailed schematic of the mold and addressing plate is given in the Supporting Information.

To fill the channels, 3.25% (w/v) SeaPrep agarose was added to HEPES buffer and melted at $T > 50$ °C. The agarose was aliquoted into eppendorf tubes and cooled to 40 °C in a dry block heating system (Grant Instruments, England). The 0.5 μm-functionalized polystyrene particles were diluted in agarose (dilution factor 1:2.6), giving final concentrations of 0.1% particles (w/v) and 2% SeaPrep agarose (w/v), respectively. A pipet was used to inject 6 μL of the particle/gel solution into each channel. The hydrogel array block was immediately submerged in HEPES and left to gel at 4 °C. The channels form a gel after 3 h; however, a longer gelation time improves the mechanical stability of the arrays. Arrays for reverse phase assays and drying experiments were cooled overnight, while arrays used for the sandwich assays were left at 4 °C for 6 h. After cooling, the hydrogel blocks were sliced perpendicular to the channels with a scalpel. As a result of manual slicing, the array thickness varied between ~1 and 2 mm.

2.3. Particle Functionalization. Polystyrene microspheres were functionalized for the reverse phase assay with either mouse or rabbit IgG and for the sandwich assay with antihuman

IgG (Fc specific). Beads coated with BSA were the negative control for both assay types. To functionalize the particles, 50 μL of the 0.5 μm beads (2.62% w/v) were washed twice in 1.5 mL of HEPES buffer by exchanging the supernatant with buffer after centrifugation. To remove the supernatant, the beads were spun down with a microcentrifuge (14 000*g*, 10 min). Following the washing, the beads were shaken overnight (1000 rpm) in 1 mL of mouse IgG (250 μg/mL), rabbit IgG (250 μg/mL), antihuman IgG (Fc specific) (220 μg/mL), or BSA (250 μg/mL). The beads were then washed two more times in 1 mL of HEPES before blocking with 10 mg/mL BSA. The incubation steps for the blocking were each 30 min of shaking at 1000 rpm (Eppendorf Thermomixer, Germany). BSA was replaced with 50 μL of buffer for storing the beads at 4 °C.

2.4. Diffusion Experiments. Fluorescence recovery after photobleaching (FRAP) was used to quantify the diffusion of IgG in 2% SeaPrep agarose. To prepare gel samples, 4% (w/v) SeaPrep agarose (prepared as described above) was mixed in equal parts with IgG-FITC (100 μg/mL) and injected into a thin chamber on a glass slide. The gelation chamber is formed by two spacers (thickness: 150 μm) and a coverslip. The gel-filled chamber was sealed and submerged in HEPES buffer for 6 h at 4 °C. The gel vertically displaced the spacers, increasing the slice thickness to ~200 μm.

Fluorescence recovery images were taken at irregular intervals after bleaching a circular area (radius: 35 μm) in an IgG-loaded gel. Bleaching was done using a Zeiss LSM 510 Confocal Laser Scanning microscope (Carl Zeiss, Germany). To form the bleached area, a 488 nm argon laser was scanned 50 times at maximum power across the region of interest. Images of fluorescent recovery after photobleaching were taken with a 40× LD Plan Neofluar objective (N.A. 0.6, optical slice 17.7 μm), with the laser power reduced to 6%. The diffusion coefficient was determined from the fractional fluorescent recovery curves, based on the theories of Axelrod (48) and Soumpasis (49). We assessed the recovery profile to ensure diffusion is predominantly two-dimensional before fitting the data. FRAP analysis was performed on six measurements from three independent experiments using ImageJ software (Image processing and analysis in Java, National Institutes of Health; http://rsb.info.nih.gov).

2.5. Microarray Assays. Array slices for the reverse phase assay were prepared with mouse IgG-, rabbit IgG-, or BSA-coated beads. The slices were incubated overnight on a flat shaker in a HEPES buffer solution containing both AlexaFluor488 antirabbit IgG (5 μg/mL) and AlexaFluor633 antimouse IgG (5 μg/mL). The arrays were quickly rinsed three times with HEPES, by injecting and removing the buffer with a pipet, and then gently shaken in 2.5 mL of buffer for 2 h.

Array slices for the sandwich assay had an alternating pattern of BSA- and antihuman IgG (Fc specific)-coated beads. The slices were incubated overnight under gentle shaking in concentrations of human IgG ranging from 0.1 pM to 10 nM. Human IgG dilutions were prepared in 100 μg/mL of BSA. Arrays were rinsed by gentle shaking in 4 mL of buffer for 2.5 h, exchanging the buffer every 30 min. The slices were incubated for 2 h in the detection antibody (5 μg/mL of antihuman IgG (Fab specific)-FITC), followed by the same rinsing procedure.

2.6. Microarray Imaging and Evaluation. Microarrays were imaged using a Zeiss LSM 510 Confocal Laser Scanning microscope. Fluorescently tagged antibodies were excited with either a 488 nm Argon laser (FITC, and AlexaFluor488) or a 633 nm Helium Neon laser (AlexaFluor633). The emission filters used were Zeiss LP505 (green) or LP650 (red). Images for determining array sensitivity were taken with a 10× EC Plan Neofluar objective (N.A. 0.3, optical slice 50.4 μm), while images of the entire array were composed from a series of images taken with a 5× objective (EC Plan Neofluar N.A. 0.16).

The signal-to-background (s/b) ratio was calculated from the mean intensity of a circular area, 500 μm in diameter and centered over the array spot, divided by the mean intensity of the background. The background was the average signal from a 0.3 mm^2 border around the image. The dose−response curve is a plot of the mean signal-to-background and standard deviation of three independent experiments. To quantitatively compare images, the detector gain, amplifier offset, laser power, and pinhole were kept constant. For each experiment, 12 microarrays were prepared from the same particle/hydrogel mixture and incubated in different antigen concentrations. The signal-to-background for each array was the average from five spot replicates. The limit of detection was determined from the average signal-to-background of the negative control (arrays incubated in BSA followed by the detection antibody) incremented by 3× the standard deviation.

2.7. Drying Experiments. The ZeptoREADER (Zeptosens, a division on Bayer (Schweiz) AG, Switzerland), a planar waveguide-based microarray reader, was used to image hydrogel microarrays as they dried and to evaluate the potential of drying as a concentration strategy.

After performing a reverse assay in solution, a gel slice was placed on a Ta_2O_5 waveguide (Zeptosens, Switerland) and imaged periodically using the red channel of the ZeptoREADER (635 nm, 3 s illumination, gray filter 1). Image analysis was done using the SensiChip View 2.1 (Zeptosens). Signal-to-noise was defined as the signal on the spot minus the background fluorescence divided by the standard deviation in the supporting agarose matrix.

3. RESULTS AND DISCUSSION

3.1. Array Preparation. We present a new method to produce multiplexed biochip copies easily and rapidly by immobilizing functionalized beads in hydrogel channels. Our microarrays consist of 25 hydrogel spots, each containing a large number of antibody-coated polystyrene microparticles. The channels are formed in agarose by molding the gel around an array of pins. SeaPrep agarose is then mixed with the particles and injected into the channels (Figure 1). These hydrogel blocks are sliced perpendicular to the channels, producing multiple copies of the microarray. After manual slicing, the 500 μm spots containing biofunctional particles were round and well-defined (Figure 2a,b).

Manual slicing meant there was limited control over array thickness, which typically ranged between 1 and 2 mm. This variation did not significantly affect array performance, as the proteins were shown to rapidly diffuse through 2% SeaPrep agarose gel (see Section 3.2). In addition, to quantitatively compare fluorescence, the arrays were imaged using an identical optical slice, which was thinner than the array.

Particles with a diameter of 0.5 μm are physically trapped in the hydrogel matrix, as demonstrated with a bleaching experiment (Figure 2). The particles did not diffuse into the bleached area during a period of 14 h, indicating that they are immobilized in the SeaPrep agarose. Even though the beads were physically trapped after only 3 h of cooling at 4 °C, we found that a longer gelation time increases the reliability of producing mechanically stable arrays. When stored in buffer, the hydrogel arrays maintained their structure for several months after preparation.

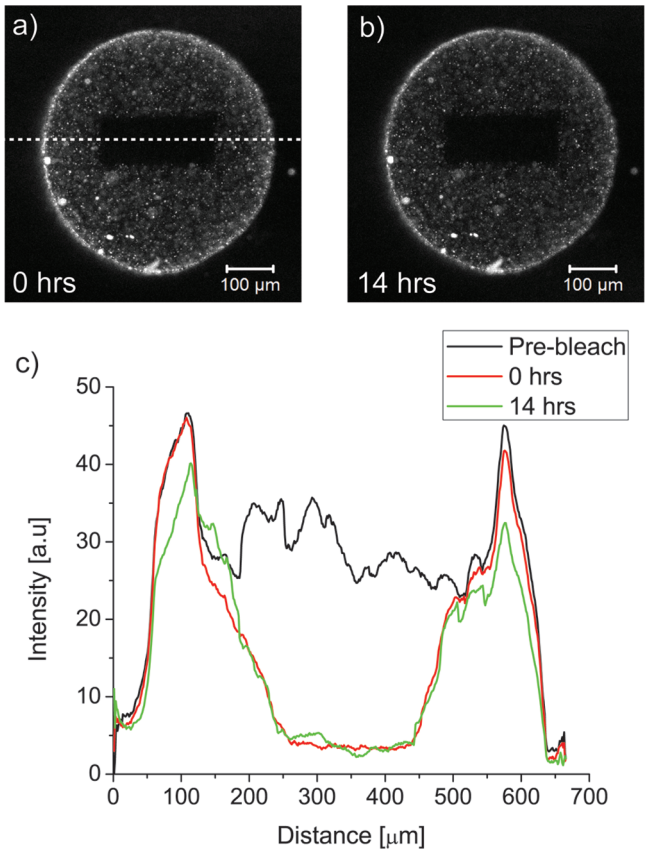

FIGURE 2. Trapping particles in 2% SeaPrep agarose. (a) The images are of a spot containing 0.5 μm beads coated with human IgG-FITC and immobilized in 2% SeaPrep agarose. The first image was taken immediately after bleaching a rectangle in the center of the array spot, (b) and the second was taken after 14 h. (c) This plot compares the intensity profiles from a spot before bleaching, immediately after bleaching, and 14 h after bleaching. The position of the line scan through the image is indicated by the dotted line in (a). The line scans clearly show that even after 14 h the beads do not diffuse into the bleached region. The intensity profile was smoothed with a moving average filter (window: 50 pix) in order to reduce the noise originating from the inhomogeneous distribution of fluorescence in the sample due to the beads.

The particle-based fabrication technique uses standard laboratory equipment and fluorescence-based read-out to create custom arrays of biomolecules. This approach is highly flexible, as protein immobilization is not restricted to any particular gel chemistry (13, 39). Several techniques have been developed for attaching proteins to microparticles, including physical adsorption, covalent coupling, and specific noncovalent attachment with affinity tags (41−43). A variety of protein-coated particles is also commercially available. In our system, capture probes are immobilized by physical adsorption. While this technique can suffer from protein leaching, low surface coverage, and random protein orientation, it remains the simplest and most flexible approach (50), and for these reasons, it is still widely used (see, e.g., refs 51−53). We have chosen this technique as a model to illustrate the flexibility of the use of microparticles as biorecognition supports. The versatility of our system comes from the ability to fill the agarose channels with a broad range of biologically relevant molecules. The particle biofunctionalization procedure can be easily altered to meet the user's needs.

With this simple fabrication technique, multiple biochip copies can be produced quickly and economically. The agarose channel support is ready in 30 min, and preparation of a block of microarrays takes less than 8 h. Gelation time is currently the limiting factor for quick array production, and further optimization could potentially further reduce fabrication time. We have produced arrays with a relatively large spot size; however, our molding approach makes it possible to easily alter the spacing, size, and number of pins, to create denser microarrays for high-throughput screening applications.

Affordable and easy to work with, agarose is ideal for the support structure because it has low fluorescent background and is mechanically stable enough to support the microchannels (10, 39). In addition, proteins can diffuse through an agarose matrix without being nonspecifically captured. The gel used to entrap particles in the channels must be injectable at room temperature with a gelation procedure that does not denature proteins. To meet these requirements, we filled the channels with a low gelation temperature agarose. SeaPrep agarose, a hydroxyethylated version of agarose, forms a gel at 18 °C, instead of 37 °C, for 2% (w/v). SeaPrep agarose was only used in the channels because hydroxyethylation also reduces the gel strength, making it unsuitable as a support structure.

We previously demonstrated that slicing a biofunctionalized hydrogel block is a simple method for producing many biochip copies (39). Layered stacks were prepared by consecutive dipping and gelation in a solution of agarose and functionalized microparticles, producing one-dimensional striped arrays. By moving from functionalized stripes to spots, we maintain the advantages of the previous system while increasing the flexibility and degree of multiplexing. The original dipping approach required a large amount of excess particles, proteins, and hydrogel. In the current system, the entire sample is available for immobilization, and the technology is easily adaptable to existing automated pipetting systems. We achieved comparable sensitivity using only 4 μL of hydrogel, with 0.1% (w/v) microparticles, in each channel. The ability to detect low analyte concentrations with minimal sample consumption is especially important in medical applications, where only limited sample quantities are available (54).

3.2. Protein Diffusion. The array spots must contain a nonfouling hydrogel with a large pore size (radius of IgG ~7 nm (55)) to ensure proteins can diffuse quickly to their capture probes. Diffusion of proteins through the hydrogel channels was tested with fluorescence recovery after photobleaching (FRAP) experiments. A typical fluorescence recovery curve is shown in Figure 3a. Full recovery was observed, indicating that no proteins were trapped in the gel. The diffusion coefficient for IgG in 2% SeaPrep agarose was found to be $1.34 \times 10^{-7} \pm 0.22 \times 10^{-7}$ cm^2/s, calculated from six fluorescence recovery curves.

These results illustrate that proteins as large as IgG readily diffuse through low concentrations of SeaPrep agarose, while larger particles remain physically immobilized. According to

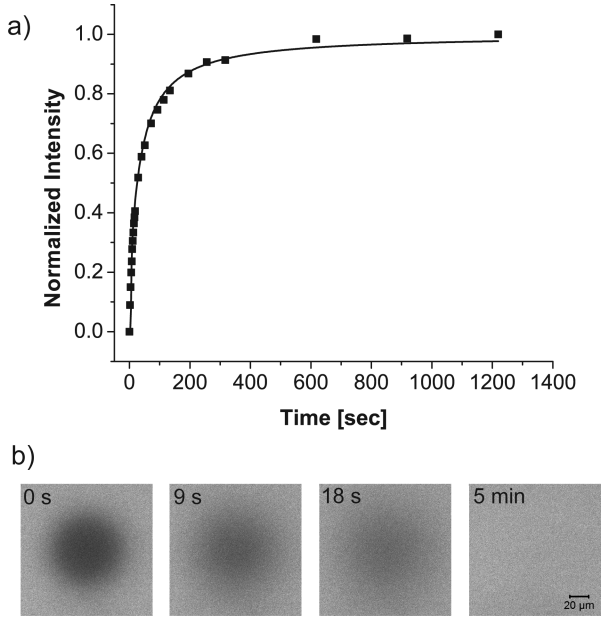

FIGURE 3. Diffusion of IgG in 2% SeaPrep agarose. (a) A typical fluorescence recovery curve. The fit is based on the equations of Axelrod (48) and Soumpasis (49). (b) Images from various stages of fluorescence recovery after bleaching a circular area (radius: 35 μm) in a thin gel slice loaded with IgG-FITC.

the literature, the pore size of agarose is typically around 100 nm. The exact value depends on the concentration, gelation conditions, gel type, and method used to determine the pore size (46, 56−58). Hydroxyethyl groups decrease the porosity of agarose; the size of the pores in 4% (w/v) SeaPrep agarose is ~42 nm (45). Despite these findings, the diffusion coefficient reported here is comparable to values found in literature for 2% agarose (2.59×10^{-7} cm^2/s) (59).

Our microarrays were sliced approximately 1 to 2 mm thick and, as a result, each array spot is a short cylinder of functionalized particles embedded in the agarose support. To demonstrate array functionality and that proteins diffuse through the gel slices, a binding experiment was performed using beads coated with antihuman IgG (Fc specific). The array slices were imaged at various depths within the gel. Figure 4a shows a schematic of a particle-loaded spot viewed from the side. Optical slices were taken at 0 and 500 μm, as indicated by the cross-sectional lines on the schematic. The strong fluorescent signal near the middle (2.2 s/b at 0 μm and 1.9 s/b at 500 μm) indicates that antibodies were able to completely diffuse through the array slices and do not only bind to capture probes on the array surface (Figure 4b,c).

3.3. Multiplexing. A model reverse phase assay was used as a proof of concept and to demonstrate the multiplexing capability of our system (Figure 5a). In a reverse phase assay, the target biomolecule is directly immobilized on the bead surface along with all other biomolecules that are present in the sample (3−5). In our model assay, IgG was the target and BSA represented the nonspecific molecules.

We injected a pattern of BSA-, rabbit IgG-, and mouse IgG-coated beads into the channels. The odd rows alternate rabbit IgG with BSA, and the even rows alternate BSA with mouse IgG. The array slices were incubated in a solution of

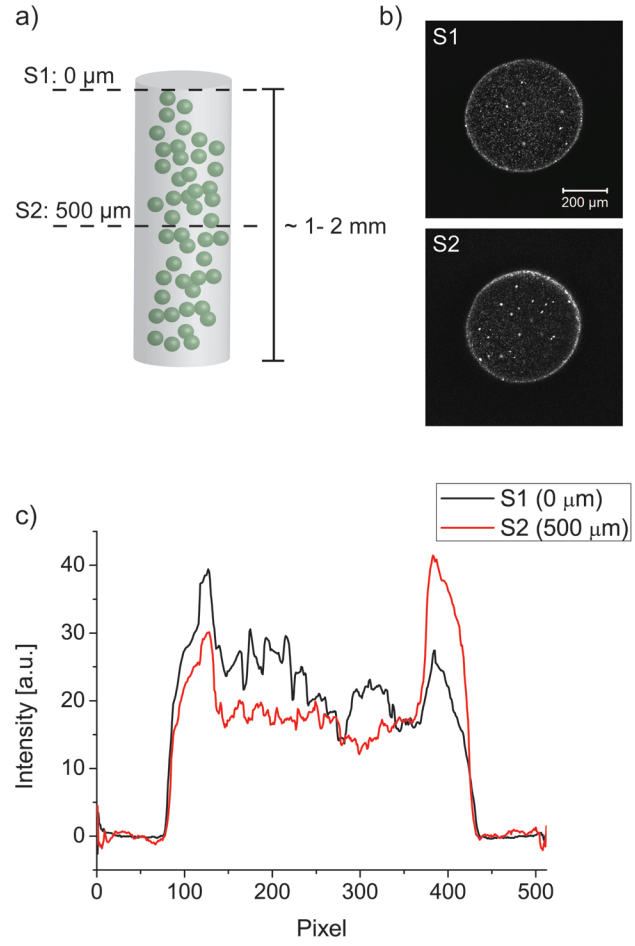

FIGURE 4. Binding experiment to test array functionality and protein diffusion. (a) A 3D schematic of a hydrogel/particle spot viewed from the side. The array slice was imaged at two depths within the gel (0 and 500 μm) to illustrate that the antibodies diffuse through the channel and do not only bind to capture probes on the surface. The beads are not drawn to scale. (b) Images of the 40.2 μm thick optical slices at positions S1 and S2. The images of the array spots are from a sandwich assay detecting 10 nM of human IgG. The s/b is 2.2 at 0 μm (S1) and 1.9 at 500 μm (S2). (c) The fluorescence intensity profile across the center of images S1 (black) and S2 (red). The plot was smoothed with a moving average filter (window: 50 pix) to minimize noise.

fluorescently labeled antimouse and antirabbit IgG. Figure 5b is an image of the reverse assay. Between each fluorescent spot is a negative control of only BSA-coated beads. The fluorescent signal was highly specific (s/b > 3), had low cross-reactivity (s/b < 1.0), and low unspecific binding on the BSA spots (s/b = 1.0).

3.4. Detection Limit. The sensitivity of the system was evaluated with a model sandwich assay for detecting human IgG (Figure 6a). Beads coated with antihuman IgG (Fc specific) and control BSA beads were arranged in a checkerboard pattern, as shown in Figure 6b. The arrays were incubated overnight in a BSA solution spiked with concentrations of human IgG ranging from 0.1 pM to 10 nM. The incubation and rinsing times were tested to ensure antibody binding reaches equilibrium and any unbound proteins are washed from the matrix before imaging (see Supporting Information). The time needed for the sandwich assay is consistent with standard assay protocols.

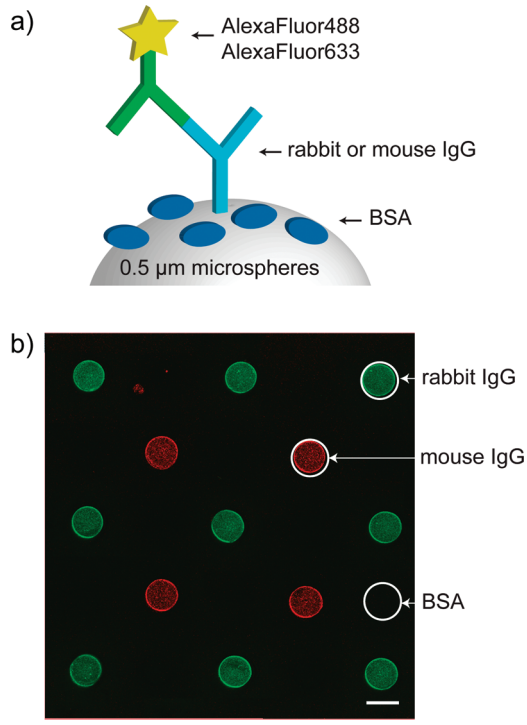

FIGURE 5. Arrays to detect rabbit and mouse IgG. (a) Schematic of the reverse phase assay. (b) Image of the array after incubation in AlexaFluor633 antimouse IgG and AlexaFluor488 antirabbit IgG solution. A checkerboard pattern was formed with IgG-coated particles and BSA-coated controls for monitoring nonspecific binding. The odd rows alternate rabbit IgG with BSA, and the even rows alternate BSA with mouse IgG. The scale bar is 500 μm.

Figure 6c is the average dose–response curve from three independent experiments. The LOD is 12 pM for the human IgG sandwich assay. This value is comparable to standard fluorescence-based immunoassays (6, 8), even though manual array preparation and bead functionalization decrease experimental reproducibility. The LOD for individual experiments is around 2 pM, representing only the variation between array spots without considering the variations due to sample handling. The fluorescent signal on the BSA beads was s/b = 0.97 ± 0.034, indicating low nonspecific binding.

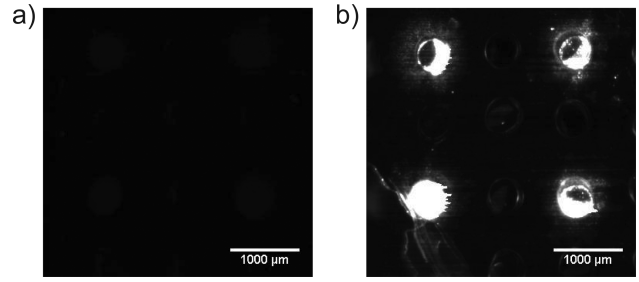

FIGURE 7. Drying the hydrogel microarrays. Red-channel (635 nm) ZeptoREADER images of an array for the detection of mouse IgG. The left image was taken directly after placing the wet array on the planar waveguide. The right image is the same sample after drying at room temperature for 100 min and was taken using the same imaging settings.

3.5. Concentrating the Sample. SeaPrep agarose channels collapse rapidly when exposed to air, but the agarose support maintains structural integrity for longer. As a result, the hydrogel slices can be intentionally dried on a solid surface, after biorecognition in an aqueous environment, to form a planar microarray, and to concentrate the sample on the surface. This strategy was evaluated using an array slice from a reverse assay (as described in Section 3.3). The slides containing BSA, rabbit IgG, and mouse IgG were incubated with fluorescently labeled antimouse IgG and imaged periodically with an evanescent field-based microarray reader while the hydrogel spots dried.

Figure 7 compares images taken before and after drying. The intensity drastically increases as the spots dry, indicating that through this process the fluorescent particles are concentrating in the evanescent field. The signal in this example increases 62 times for the four spots of fluorescent microparticles, resulting in an increase in s/n by a factor of 1.9 (signal from 784 ± 181 to 48800 ± 9070, s/n from 11.9 ± 4.8 to 22.5 ± 2.2). The signal of the nonfluorescent BSA controls was comparable to the background value.

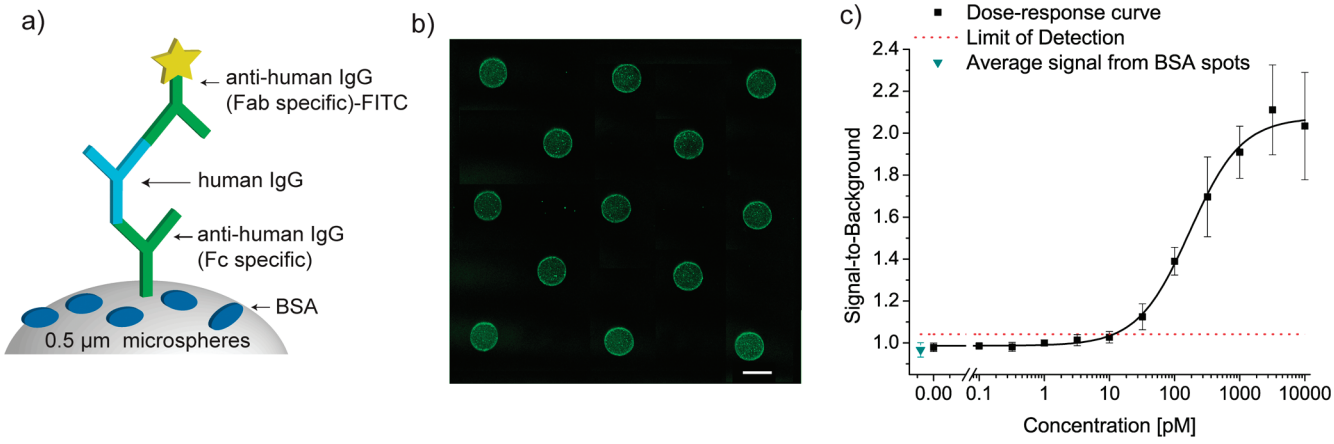

FIGURE 6. Sandwich assay for detecting human IgG. (a) Schematic of the sandwich assay. (b) Image of an array after incubation in 3.2 nM human IgG and 33.3 nM antihuman IgG (Fab specific)-FITC. Channels with IgG-coated beads alternate with channels of BSA-coated beads to form a checkerboard pattern. The scale bar is 500 μm. (c) Dose–response curve for a model sandwich assay to detect human IgG. The curve is the average of three independent experiments. The hydrogel/particle mixture used to form the spots is the same for all slices in a given experiment. The mean signal-to-background for each slice is the average of five spots. The red dotted line is used to determine the limit of detection and is calculated from the signal-to-background for 0 pM incremented by 3× its standard deviation. The green triangle shows the average signal on BSA-coated beads, indicating very low nonspecific binding.

Images were taken with the ZeptoREADER, a microarray reader based on planar waveguide technology, which uses high illumination intensity to detect fluorescent molecules within the evanescent field (~200 nm). The ZeptoREADER achieves signal-to-noise ratios up to 78 times higher than a confocal scanner (60). However, because of this thin optical slice, it is important to pack a large number of fluorescent probes very near the surface. The particles in our hydrogel microarrays are initially immobilized throughout a gel slice ~10 000 times thicker than the optical slice of the ZeptoREADER. This means that the hydrogel slices are initially too thick to take advantage of this sensitivity and only a few fluorescent molecules can be detected before drying.

By concentrating the fluorescent probes from a gel slice into the evanescent field, we make our hydrogel-based approach compatible with highly sensitive evanescent field-based devices. As this imaging approach does not affect array fabrication, custom arrays are still produced rapidly and can be stored for extended periods before drying. In addition to the increased fluorescent signal, we also observed an increase in background noise, which can be associated with scattering and inhomogeneity of the dried gel due to pore formation. Optimizing the concentration and type of hydrogel could lead to further improvements of the sensitivity but was beyond the scope of this work.

4. CONCLUSIONS AND OUTLOOK

We demonstrated a simple and inexpensive method for producing multiple copies of hydrogel microarrays. Arrays were fabricated without any special instrumentation and reached limits of detection comparable to standard fluorescence-based immunoassays.

SeaPrep agarose is compatible with our system because it has low nonspecific binding, is injectable at room temperature, does not denature proteins during gelation, and has a pore size that permits biomolecular diffusion while physically trapping microparticles. Nevertheless, the technique we presented is not restricted to thermoreversible gels. Protein resistant photo- or chemically cross-linkable gels with a sufficient pore size could replace agarose in the channels to reduce array preparation time (e.g., alginate (61) or polyacrylamide-based gels (10)). With these modifications, proteins could also be directly coupled to the gel matrix, as an alternative to microparticles as the supports for biorecognition.

For high throughput and automated assays, it is important that the array slices are identical. Being able to slice the gel block reliably into thin (<1 mm) arrays increases the yield, reduces scattering, and minimizes excess material (i.e., when the array slice is several times thicker than the optical slice). For example, slicing hydrogels with a microtome would produce thin but fragile array slices of controlled thickness. By embedding the hydrogel channels into a stronger, nonpermeable support (e.g., polydimethylsiloxane (PDMS)), the sliced arrays would be easier to handle. The PDMS would also facilitate denser array fabrication by stacking structures of periodic trenches to form the microchannels obtained with conventional photolithography methods.

We are currently working on integrating a flow-through system for rapid assay analysis using minute sample volumes. For hydrogel-based arrays, accelerating the reaction–diffusion kinetics will significantly shorten the analysis times (62). Flow-through analysis would allow spots to be addressed individually, further increasing the flexibility. This can be combined with optimizing microparticle size and concentration to further improve the limit of detection. In this paper, we chose a low concentration of particles, producing arrays with acceptable sensitivity and minimal protein consumption. Depending on the how much sample is available for particle functionalization, the particle concentration could be increased, potentially resulting in better signal-to-noise ratios.

We presented a fabrication method that makes protein microarrays more accessible by eliminating the need for costly machinery. Our system is highly flexible; a wide range of biological molecules can be immobilized in the channels to create multiple copies of custom arrays. The ability to rapidly produce cheap, sensitive, and flexible arrays is important for any high-throughput application, and we believe this approach has great potential as an alternative to traditional robotic spotting and lithographic techniques.

Acknowledgment. The authors would like to thank the ETH Zurich and the National Sciences and Engineering Research Council of Canada for funding.

Supporting Information Available: Schematic of the mold and addressing plate for array fabrication and rinsing optimization experimental results. This material is available free of charge via the Internet at http://pubs.acs.org.

REFERENCES AND NOTES

(1) LaBaer, J.; Ramachandran, N. *Curr. Opin. Chem. Biol.* **2005**, *9*, 14–19.
(2) Templin, M. F.; Stoll, D.; Schrenk, M.; Traub, P. C.; Vohringer, C. F.; Joos, T. O. *Trends Biotechnol.* **2002**, *20*, 160–166.
(3) Joos, T.; Bachmann, J. *Front. Biosci.* **2009**, *14*, 4376–4385.
(4) Hartmann, M.; Roeraade, J.; Stoll, D.; Templin, M.; Joos, T. *Anal. Bioanal. Chem.* **2009**, *393*, 1407–1416.
(5) Hall, D. A.; Ptacek, J.; Snyder, M. *Mech. Ageing Dev.* **2007**, *128*, 161–167.
(6) Bally, M.; Halter, M.; Voros, J.; Grandin, H. M. *Surf. Interface Anal.* **2006**, *38*, 1442–1458.
(7) Caiazzo, R. J.; Maher, A. J.; Drummond, M. P.; Lander, C. I.; Tassinari, O. W.; Nelson, B. P.; Liu, B. C. S. *Proteomics: Clin. Appl.* **2009**, *3*, 138–147.
(8) Lee, H. J.; Wark, A. W.; Corn, R. M. *Analyst* **2008**, *133*, 975–983.
(9) Zhang, S. G. *Nat. Mater.* **2004**, *3*, 7–8.
(10) Rubina, A. Y.; Kolchinsky, A.; Makarov, A. A.; Zasedatelev, A. S. *Proteomics* **2008**, *8*, 817–831.
(11) Olle, E. W.; Messamore, J.; Deogracias, M. P.; McClintock, S. D.; Anderson, T. D.; Johnson, K. J. *Exp. Mol. Pathol.* **2005**, *79*, 206–209.
(12) Angenendt, P. *Drug Discovery Today* **2005**, *10*, 503–511.
(13) Stevens, P. W.; Wang, C. H. J.; Kelso, D. M. *Anal. Chem.* **2003**, *75*, 1141–1146.
(14) Zubtsov, D. A.; Savvateeva, E. N.; Rubina, A. Y.; Pan'kov, S. V.; Konovalova, E. V.; Moiseeva, O. V.; Chechetkin, V. R.; Zasedatelev, A. S. *Anal. Biochem.* **2007**, *368*, 205–213.
(15) Stillman, B. A.; Tonkinson, J. L. *BioTechniques* **2000**, *29*, 630–635.
(16) Marsden, D. M.; Nicholson, R. L.; Ladlow, M.; Spring, D. R. *Chem. Commun. (Cambridge, U.K.)* **2009**, *7107*, 7109.
(17) Preininger, C.; Sauer, U.; Obersriebnig, S.; Trombitas, M. *Int. J. Environ. Anal. Chem.* **2005**, *85*, 645–654.

(18) Goldman, E. R.; O'Shaughnessy, T. J.; Soto, C. M.; Patterson, C. H.; Taitt, C. R.; Spector, M. S.; Charles, P. T. *Anal. Bioanal. Chem.* **2004**, *380*, 880–886.
(19) Charles, P. T.; Goldman, E. R.; Rangasammy, J. G.; Schauer, C. L.; Chen, M. S.; Taitt, C. R. *Biosens. Bioelectron.* **2004**, *20*, 753–764.
(20) Bhatnagar, P. *Appl. Phys. Lett.* **2007**, *91*, 3.
(21) Derwinska, K.; Sauer, U.; Preininger, C. *Talanta* **2008**, *77*, 652–658.
(22) Derwinska, K.; Gheber, L. A.; Preininger, C. *Anal. Chim. Acta* **2007**, *592*, 132–138.
(23) Zhou, Y.; Andersson, O.; Lindberg, P.; Liedberg, B. *Microchim. Acta* **2004**, *147*, 21–30.
(24) Afanassiev, V.; Hanemann, V.; Wolfl, S. *Nucleic Acids Res.* **2000**, *28*, 5.
(25) Angenendt, P.; Glokler, J.; Murphy, D.; Lehrach, H.; Cahill, D. J. *Anal. Biochem.* **2002**, *309*, 253–260.
(26) Charles, P. T.; Taitt, C. R.; Goldman, E. R.; Rangasammy, J. G.; Stenger, D. A. *Langmuir* **2004**, *20*, 270–272.
(27) Guschin, D.; Yershov, G.; Zaslavsky, A.; Gemmell, A.; Shick, V.; Proudnikov, D.; Arenkov, P.; Mirzabekov, A. *Anal. Biochem.* **1997**, *250*, 203–211.
(28) Arenkov, P.; Kukhtin, A.; Gemmell, A.; Voloshchuk, S.; Chupeeva, V.; Mirzabekov, A. *Anal. Biochem.* **2000**, *278*, 123–131.
(29) Kim, D. N.; Lee, W.; Koh, W. G. *Anal. Chim. Acta* **2008**, *609*, 59–65.
(30) Saaem, I.; Papasotiropoulos, V.; Wang, T.; Soteropoulos, P.; Libera, M. *J. Nanosci. Nanotechnol.* **2007**, *7*, 2623–2632.
(31) Chen, L.; Chen, Z. T.; Wang, J.; Xiao, S. J.; Lu, Z. H.; Gu, Z. Z.; Kang, L.; Chen, J.; Wu, P. H.; Tang, Y. C.; Liu, J. N. *Lab Chip* **2009**, *9*, 756–760.
(32) Andersson, O.; Larsson, A.; Ekblad, T.; Liedberg, B. *Biomacromolecules* **2009**, *10*, 142–148.
(33) Choi, D.; Jang, E.; Park, J.; Koh, W. G. *Microfluid. Nanofluid.* **2008**, *5*, 703–710.
(34) Kim, D. N.; Lee, Y.; Koh, W. G. *Sens. Actuators, B: Chem.* **2009**, *137*, 305–312.
(35) Darii, E.; Lebeau, D.; Papin, N.; Rubina, A. Y.; Stomakhin, A.; Tost, J.; Sauer, S.; Savvateeva, E.; Dementieva, E.; Zasedatelev, A.; Makarov, A. A.; Gut, I. G. *New Biotechnol.* **2009**, *25*, 404–416.
(36) Dyukova, V. I.; Dementieva, E. I.; Zubtsov, D. A.; Galanina, O. E.; Bovin, N. V.; Rubina, A. Y. *Anal. Biochem.* **2005**, *347*, 94–105.
(37) Kiyonaka, S.; Sada, K.; Yoshimura, I.; Shinkai, S.; Kato, N.; Hamachi, I. *Nat. Mater.* **2004**, *3*, 58–64.
(38) Tanaka, H.; Hanasaki, M.; Isojima, T.; Takeuchi, H.; Shiroya, T.; Kawaguchi, H. *Colloids Surf., B: Biointerfaces* **2009**, *70*, 259–265.
(39) Bally, M.; Voros, J.; Takeuchi, S. *Lab Chip* **2010**, *10*, 372—378.
(40) Drahoslav, L.; Anderson, N. G.; Braatz, J. A. Microarray channel devices produced by a block mold process [Online]. US Patent 0203366, Oct. 30, 2003. http://www.freepatentsonline.com/20030203366.pdf (accessed Dec. 2, 2010).
(41) Meza, M. B. *Drug Discovery Today* **2000**, *38*, 41.
(42) Verpoorte, E. *Lab Chip* **2003**, *3*, 60N–68N.
(43) Nolan, J. P.; Sklar, L. A. *Trends Biotechnol.* **2002**, *20*, 9–12.
(44) Joos, T. O.; Stoll, D.; Templin, M. F. *Curr. Opin. Chem. Biol.* **2002**, *6*, 76–80.
(45) Renn, D. W. *Ind. Eng. Chem. Prod. Res. Dev.* **1984**, *23*, 17–21.
(46) Stellwagen, N. C. *Electrophoresis* **2009**, *30*, S188–S195.
(47) Meilander, N. J.; Yu, X. J.; Ziats, N. P.; Bellamkonda, R. V. *J. Controlled Release* **2001**, *71*, 141–152.
(48) Axelrod, D.; Koppel, D. E.; Schlessinger, J.; Elson, E.; Webb, W. W. *Biophys. J.* **1976**, *16*, 1055–1069.
(49) Soumpasis, D. M. *Biophys. J.* **1983**, *41*, 95–97.
(50) http://www.polysciences.com/SiteData/poly/Assets/DataSheets/410.pdf.
(51) Lucas, L. J.; Chesler, J. N.; Yoon, J. Y. *Biosens. Bioelectron.* **2007**, *23*, 675–681.
(52) Sato, K.; Tokeshi, M.; Kimura, H.; Kitamori, T. *Anal. Chem.* **2001**, *73*, 1213–1218.
(53) McHugh, T. M.; Wang, Y. J.; Chong, H. O.; Blackwood, L. L.; Stites, D. P. *J. Immunol. Methods* **1989**, *116*, 213–219.
(54) Birtwell, S.; Morgan, H. *Integr. Biol.* **2009**, *1*, 345–362.
(55) Norde, W. *Surf. Chem. Biomed. Environ. Sci.* **2006**, *228*, 159–176.
(56) Pernodet, N.; Maaloum, M.; Tinland, B. *Electrophoresis* **1997**, *18*, 55–58.
(57) Narayanan, J.; Xiong, J. Y.; Liu, X. Y. *Int. Conf. Mater. Adv. Technol. (ICMAT 2005)* **2006**, *28*, 83–86.
(58) Aymard, P.; Martin, D. R.; Plucknett, K.; Foster, T. J.; Clark, A. H.; Norton, I. T. *Biopolymers* **2001**, *59*, 131–144.
(59) Li, R. H.; Altreuter, D. H.; Gentile, F. T. *Biotechnol. Bioeng.* **1996**, *50*, 365–373.
(60) Pawlak, M.; Schick, E.; Bopp, M. A.; Schneider, M. J.; Oroszlan, P.; Ehrat, M. *Proteomics* **2002**, *2*, 383–393.
(61) Kuo, C. K.; Ma, P. X. *Biomaterials* **2001**, *22*, 511–521.
(62) Zubtsov, D. A.; Ivanov, S. M.; Rubina, A. Y.; Dementieva, E. I.; Chechetkin, V. R.; Zasedatelev, A. S. *J. Biotechnol.* **2006**, *122*, 16–27.

AM100849F